

[Fe^{III}(tmdta)]⁻ –twist-boat/half-chair conformer ratio reliably deduced from DFT-calculated Raman spectra

Roland Meier,^{a,*} Joachim Maigut,^a Bernd Kallies,^{b,*} Nicolai Lehnert,^{c,*} Florian Paulat,^c Frank W. Heinemann,^a Gernot Zahn,^d Martin P. Feth,^e Harald Krautschäid^f and Rudi van Eldik^a

^a Institute for Inorganic Chemistry, University of Erlangen-Nürnberg, Egerlandstr. 1, 91058 Erlangen, Germany.

^b Zuse Institute Berlin, Takustr. 7, 14195 Berlin, Germany.

^c Department of Chemistry, The University of Michigan, 930 N. University, Ann Arbor, Mi 47109, USA.

^d MPI für Chemische Physik fester Stoffe, Nöthnitzer Str. 40, 01187 Dresden, Germany.

^e ALTANA Pharma AG, A Member of the NYCOMED Group, Physicochemical Research, Byk-Gulden-Str. 2, 78467 Konstanz, Germany.

^f Institute of Inorganic Chemistry, University of Leipzig, Johannisallee 29, 04103 Leipzig, Germany.

1. Experimental Methods

1.1. Chemicals and Preparation of Complexes

Materials. H₄tmdta was prepared according to literature methods¹ or purchased from Sigma-Aldrich. All other chemicals used had the highest purity commercially available and were used as received.

1.1.1. Preparation of Li[Fe(tmdta)]·3H₂O (**1a**)

The lithium salt was prepared in the same way as described above for the guanidinium salt except that two 0.01 mol (1.48 g) portions of Li₂CO₃ (Acros) were used instead of the guanidinium carbonate. The clear dark-brown reaction mixture resulting after addition of the second carbonate addition was layered with the two-fold volume of acetone and placed into a refrigerator. Yellow crystals suitable for x-ray structure analysis formed directly after three days.

Results Li[Fe(tmdta)]·3H₂O (**1c**) (yield 3.50 g; 66 %). *Anal.* Calcd C₁₁H₂₀FeLiN₂O₁₁ (419.1 g/mol): C, 31.53; H, 4.81; N, 6.68. Found: C, 31.44; H, 4.77; N, 6.71.

1.1.2. Preparation of NH₄[Fe(tmdta)]·0.5H₂O (**1b**).

The ammonium salt was again prepared analogously as described above for the guanidinium and lithium salts except that two 0.02 mol (1.58 g) portions of (NH₄)HCO₃ (Acros) were used instead of guanidinium and lithium carbonates. The clear dark-brown reaction mixture resulting after addition of the second ammonium bicarbonate addition was layered with the three-fold volume of acetone and placed into a refrigerator. Yellow crystals suitable for x-ray structure analysis formed directly after ten days. *Anal.* Calcd C₁₁H₁₉FeN₃O_{8.5} (385.1 g/mol): C, 34.30; H, 4.97; N, 10.91. Found: C, 34.26; H, 5.00; N, 10.89.

*1.1.3. Preparation of Na[Fe(tmdta)]·3H₂O (**1c**).*

To a suspension of H₄tmdta (3.06 g, 0.01 mol) in 20 ml of water, 1.68 g (0.02 mol) of NaHCO₃ were added with stirring. After the resulting solution became clear, 5.16 g (0.01 mol) of [Fe(H₂O)₆](ClO₄)₃·3H₂O² (Alfa Aesar) were poured into the previous solution. When the carbon dioxide development was over, another portion of 1.68 g (0.02 mol) of NaHCO₃ were added with continuous stirring. The resulting deep brown solution must have a pH between 5 and 6. The mixture was layered with an threefold volume of acetone and placed in a refrigerator. Clear yellow crystals are formed within four days.

Results: Na[Fe(tmdta)]·3H₂O (**1c**) (yield 3.50 g; 80 %). *Anal.* Calcd C₁₁H₂₀FeN₂NaO₁₁ (435.1 g/mol): C, 30.36; H, 4.63; N, 6.44. Found: C, 30.25; H, 4.58; N, 6.39.

*1.1.4. Preparation of K[Fe(tmdta)] (**1d**).*

To a suspension of H₄tmdta (3.06 g, 0.01 mol) in 20 ml of water, 2.0 g (0.02 mol) of KHCO₃ were added with stirring. After the resulting solution became clear, 4.04 g (0.01 mol) [Fe(H₂O)₆](NO₃)₃·3H₂O (Acros) were poured into the previous solution. When the carbon dioxide development has ceased, another 2.0 g (0.02 mol) of KHCO₃ were added with continuous stirring. The resulting deep red-brown solution must have a pH between 5 and 6. The mixture was layered with an equivalent volume of acetone and placed in a refrigerator. Clear yellow crystals of x-ray diffraction quality are formed within one week.

Results: K[Fe(tmdta)] (**1d**) (yield 2.82 g; 71 %). *Anal.* Calcd C₁₁H₁₄FeKN₂O₈ (397.2 g/mol): C, 33.26; H, 3.55; N, 7.05. Found: C, 33.10; H, 3.60; N, 7.07.

*1.1.5. Preparation of {C(NH₂)₃}·[Fe(tmdta)]·2H₂O (**1e**).*

To a suspension of H₄tmdta (3.06 g, 0.01 mol) in 20 ml of water, 1.83 g (0.01 mol) of {C(NH₂)₃}₂CO₃ (Acros) were added with stirring. After the resulting solution became clear, 5.16 g (0.01 mol) of [Fe(H₂O)₆](ClO₄)₃·3H₂O² (Alfa Aesar) were poured into the previous solution. When the carbon dioxide development has ceased, another 1.83 g (0.01 mol) of {C(NH₂)₃}₂CO₃ were added with continuous stirring. The resulting deep brown solution was placed in a refrigerator. Clear yellow crystals of x-ray diffraction quality are formed within three days.

Results {C(NH₂)₃}·[Fe(tmdta)]·2H₂O (**1e**) (yield 3.00 g; 66 %). *Anal.* Calcd C₁₂H₂₄FeN₅O₁₀ (454.2 g/mol): C, 31.73; H, 5.33; N, 15.42. Found: C, 31.80; H, 5.30; N, 15.30.

1.2. Crystal structure analysis

An overview concerning the basic crystallographic parameters of the four structure determinations carried out in the present work is given in Table S1. Details of structures **1a** and **1b** have reported before. However, the new refinements done by us improved the precision in both cases considerably (**1a**: from R = 4.90 % (old)⁴ to R = 3.99%; **1b**: from R = 8.10 % (old)^{5a} to R = 4.32% (cf. table S1)).

Table S1. Crystal Data and details of the structure determinations for Li[Fe(tmdta)]·3H₂O (**1a**), NH₄[Fe(tmdta)]·0.5H₂O (**1b**), K[Fe(tmdta)] (**1d**) and {C(NH₂)₃} [Fe(tmdta)]·2H₂O (**1e**).

	1a	1b	1d	1e
Empirical formula	C ₁₁ H ₂₀ FeLiN ₂ O ₁₁	C ₁₁ H ₁₉ FeN ₃ O _{8.5}	C ₁₁ H ₁₄ FeKN ₂ O ₈	C ₁₂ H ₂₄ FeN ₅ O ₁₀
Formula weight	419.08	385.14	397.19	454.21
Crystal color, form	yellow, block	yellow, plate	yellow, block	yellow, cube
Crystal system	monoclinic	monoclinic	monoclinic	monoclinic
Space group	P2 ₁ /n (No. 14)	P2 ₁ /n (No. 14)	P2 ₁ /c (No. 14)	P2 ₁ /c (No. 14)
Unit cell dimensions				
<i>a</i> (Å)	8.888(2)	8.6446(13)	8.7684(7)	8.8188(4)
<i>b</i> (Å)	10.284(3)	11.0545(10)	12.4703(7)	10.6119(6)
<i>c</i> (Å)	17.782(5)	16.837(3)	12.8511(10)	19.6967(12)
α (°)	90	90	90	90
β (°)	95.87(2)	103.859(9)	97.577(6)	93.060(3)
γ (°)	90	90	90	90
<i>Z</i>	4	4	4	4
<i>V</i> (Å ³)	1616.8(8)	1562.1(4)	1392.9 (2)	1840.67(17)
Crystal dimensions (mm)	0.70 x 0.40 x 0.20	0.13 x 0.55 x 0.70	0.22 x 0.26 x 0.33	0.64 x 0.64 x 0.76
<i>d</i> _{calc} (g cm ⁻³)	1.722	1.638	1.894	1.639
T _{meas} (K)	295(2)	293(2)	100(2)	298(2)
Absorption coefficient, μ , (mm ⁻¹)	0.997	1.015	1.428	0.884
Radiation, λ (Å)	0.71073	0.71073	0.71073	0.71073
θ -Range	2.29-30.00	2.22-27.45	5.32-29.00	2.07-28.01
No. refl. coll.	5652	3573	12562	4445
No. refl. unique	4713	3573	3661	4445
No. refl. obs. [$F_o > 4\sigma(F)$]	3411	2094	3395	4134
refined parameters (<i>p</i>)	312	236	209	273
Abs. corr. T_{\min} / T_{\max}	0.307/0.367	0.5045/0.8764	0.617/0.796	0.5332/0.6017
R_1 ^a (observed reflections)	0.0399	0.0468	0.0215	0.0332
wR ₂ ^b (all data)	0.1037	0.1163	0.0584	0.0974
Goodness-of-fit on F^2	0.992	1.01	1.05	1.12

^a $R_1 = \Sigma|F_0| - |F_c|/\Sigma|F_0|$.

^b wR₂ = $[\Sigma[w(F_0^2 - F_c^2)^2]/\Sigma(F_0^2)]^{1/2}$; $w = 1/[\sigma^2(F_0^2) + (0.0605P)^2 + 0.0000P]$ (**1a**),

^b wR₂ = $[\Sigma[w(F_0^2 - F_c^2)^2]/\Sigma(F_0^2)]^{1/2}$; $w = 1/[\sigma^2(F_0^2) + (0.0424P)^2 + 0.1653P]$ (**1b**),

^b wR₂ = $[\Sigma[w(F_0^2 - F_c^2)^2]/\Sigma(F_0^2)]^{1/2}$; $w = 1/[\sigma^2(F_0^2) + (0.0267P)^2 + 0.6494P]$ (**1d**),

^b wR₂ = $[\Sigma[w(F_0^2 - F_c^2)^2]/\Sigma(F_0^2)]^{1/2}$; $w = 1/[\sigma^2(F_0^2) + (0.0540P)^2 + 0.8200P]$ (**1e**),

where $P = (F_0^2 + 2F_c^2)/3$.

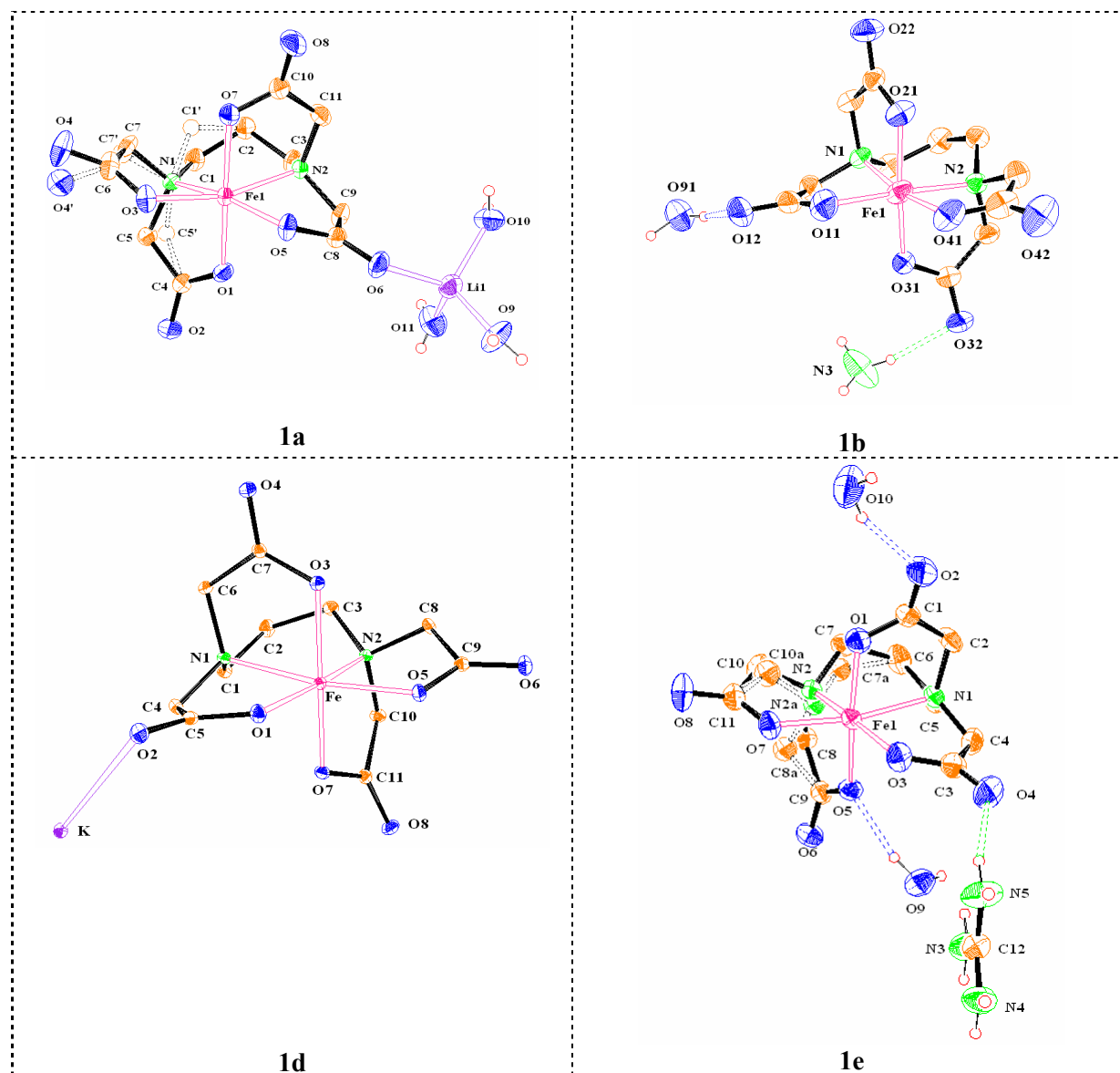


Fig. S1. Asymmetric units found during structure determinations of $\text{Li}[\text{Fe}(\text{tmdta})] \cdot 3\text{H}_2\text{O}$ (**1a**), $\text{NH}_4[\text{Fe}(\text{tmdta})] \cdot 0.5\text{H}_2\text{O}$ (**1b**), $\text{K}[\text{Fe}(\text{tmdta})]$ (**1d**) and $\{\text{C}(\text{NH}_2)_3\}[\text{Fe}(\text{tmdta})] \cdot 2\text{H}_2\text{O}$ (**1e**). The bonds in the disordered parts of structures **1a** and **1e** are shown as dotted lines. Hydrogen bonds in which crystal water molecules are involved are shown as blue dotted lines while these where guanidinium and ammonium ions are involved are depicted as green dotted lines. The Δ enantiomers are shown in the case of **1b** and **1d** while the Δ antipodes are presented for **1a** and **1e**. Because all salts crystallize in centrosymmetric space groups, the mirror images are also present with 50%.

1.2.1. $\text{Li}[\text{Fe}^{III}(\text{tmdta})] \cdot 3\text{H}_2\text{O}$ (**1a**)

The crystals of the lithium salt **1c** deliver another example how the labile $[\text{tb}] \rightleftharpoons [\text{hc}]$ equilibrium does continue its influence from the liquid into the solid phase. In difference to the situation with **1b**, there is now an overwhelming dominance of the **hc** over the **tb** form with a distribution of 91 % **hc** vs. 9 % **tb**.

1.2.2. $\text{NH}_4[\text{Fe}^{\text{III}}(\text{tmdta})] \cdot 0.5\text{H}_2\text{O}$ (**1b**)

In the previous trial to estimate the structure of the ammonium salt **1b**, some problems encountered during the refinement procedure led to an comparatively large $R = 8.10\%$.⁵ We suspect that difficulties met by Anderegg et al.⁵ were related to the single crystal water molecule in the asymmetric unit of **1b**. Our analysis showed that the occupation factor of this water is only 0.5 such that the exact formula of **1b** is that of a hemihydrate as confirmed also by the data for the elemental analysis of **1b**.

1.2.3. $\text{K}[\text{Fe}(\text{tmdta})]$ (**1d**)

The refinement of this structure led to the most precise ($R_1 = 2.15\%$) structure determination of the whole series. **1a** (cf. Fig. S1) is the only salt of the current work that doesn't contain any water of crystallization which differs e.g. to $\text{K}[\text{Co}(\text{tmdta})] \cdot 2\text{H}_2\text{O}$.³

1.2.4. $\{\text{C}(\text{NH}_2)_3\}[\text{Fe}^{\text{III}}(\text{tmdta})] \cdot 2\text{H}_2\text{O}$ (**1e**)

As mentioned in the main body of this communication, the **tb** conformation is present with 94 % of $[\text{Fe}^{\text{III}}(\text{tmdta})]^-$ in the crystals of **1b** and a 6 % fraction is concurrently formed with **hc** conformation caused by disorder in the crystal. The observation of the two different conformations in the same crystal delivers - according to our views- a tantalizing hint for the high conformational flexibility in the chelate backbone of the $[\text{Fe}^{\text{III}}(\text{tmdta})]^-$ complex and a rather low barrier of the $[\text{tb}] \rightleftharpoons [\text{hc}]$ interconversion.

Table S2 shows a collection of important Fe^{III} -donor atom distances and important valence angles defining the the FeN_2O_4 donor atom sets in **1a – 1e**. For the sake of clarity, the donor atom types have been assigned as suggested by Hoard et al.⁶ for MN_2O_4 donor atom sets in edta-type complexes where in-plane oxygen donor atoms are indexed as O_G while the out-of-plane counter parts are called O_R .

The averaged $(\text{Fe}^{\text{III}}-\text{N})_{\text{av}}$ bond length are typical for six-coordinate high spin ferric centers⁷ and virtually identical if the various standard deviations are considered ($(\text{Fe}^{\text{III}}-\text{N})_{\text{av}} = 2.197(12)$ Å for **1d**, 2.195(16) Å for **1e**, 2.192(22) Å for **1a** and 2.190(14) Å for **1b**). The average in-plane bond length $(\text{Fe}^{\text{III}}-\text{O}_G)_{\text{av}}$ is very similar between the three **tb** structure ($(\text{Fe}^{\text{III}}-\text{O}_G)_{\text{av}} = 1.963(5)$ Å for **1d**, 1.964(17) Å for **1e**, and 1.956(13) Å for **1b**) whereas this mean distance is slightly longer in ($(\text{Fe}^{\text{III}}-\text{O}_G)_{\text{av}} = 1.987(15)$ Å) of **hc** structure **1a**. The averaged out-of-plane bond lengths ($(\text{Fe}^{\text{III}}-\text{O}_R)_{\text{av}} = 1.983(6)$ Å for **1d**, 1.977(5) Å for **1e**, 1.989(5) Å for **1a**, and 1.992(1) Å for **1b**) in the 4 structures are closer to each other and slightly longer than the analogous in-plane distances (exception is again **hc** structure **1a** where $(\text{Fe}^{\text{III}}-\text{O}_G)_{\text{av}}$ is nearly identical with $(\text{Fe}^{\text{III}}-\text{O}_R)_{\text{av}}$).

The bond angles listed in Table S2 confirm the high degree of angular distortion usually met in structures of high spin Fe^{III} complexes which gets easily evident by angles along the Cartesian axis ($\text{N}_1\text{-Fe-O}_{G2}$, $\text{N}_2\text{-Fe-O}_{G1}$, and $\text{O}_{R1}\text{-Fe-O}_{R2}$) which are all about 10° smaller than the ideal value of 180° (exception is again $(\text{O}_{R1}\text{-Fe-O}_{R2}) = 175.53(7)$ ° in the **hc** structure **1a**).

Table S2. Bond lengths (\AA) and angles ($^\circ$) defining the FeN_2O_4 donor atom sets in **1a – 1e**.
 Data for **1c** from ref. ^{5b}.

	1a	1b	1c	1d	1e
Fe-N ₁	2.2079(18)	2.181(2)	2.173(2)	2.1886(9)	2.1832(13)
Fe-N ₂	2.1765(18)	2.200(3)	2.177(2)	2.2056(9)	2.2058(16)
Fe-O _{G1}	1.9763(17)	1.947(3)	1.959(2)	1.9598(8)	1.9518(13)
Fe-O _{G2}	1.9970(16)	1.968(3)	1.980(2)	1.9663(8)	1.9765(12)
Fe-O _{R1}	1.9855(16)	1.990(3)	1.971(2)	1.9789(8)	1.9729(13)
Fe-O _{R2}	1.9922(16)	1.992(3)	1.981(2)	1.9869(8)	1.9805(12)
N ₁ -Fe-N ₂	94.23(7)	89.97(9)	92.1(1)	88.13(3)	90.91(6)
N ₁ -Fe-O _{G1}	77.80(7)	82.02(10)	80.1(1)	81.35(3)	81.70(5)
N ₂ -Fe-O _{G2}	78.77(7)	81.33(10)	82.7(1)	80.73(3)	80.02(6)
O _{G1} -Fe-O _{G2}	112.51(7)	107.49(11)	105.8(1)	109.94(3)	108.50(6)
N ₁ -Fe-O _{G2}	163.80(7)	168.89(11)	170.6(1)	167.76(3)	168.47(5)
N ₂ -Fe-O _{G1}	163.29(7)	168.96(10)	167.7(1)	168.73(3)	167.09(6)
O _{R1} -Fe-O _{R2}	175.53(7)	169.02(9)	169.9(1)	168.00(3)	171.18(6)

1.3. Raman Spectra

1.3.1. Solid State Spectra

Raman spectra of solid samples were obtained on a setup that consists of the following components: an Acton SpectraPro 500-i double monochromator with an attached PI-CCD camera (1100 x 330 pixel, back illuminated with UVAR coating), and a Spectra-Physics Stabilite 2017 Ar⁺ ion gas laser. Measurements were performed on solids cooled to liquid nitrogen temperature. The excitation wavelength was set to 514 nm with an energy of 25 – 50 mW.

1.3.2. Solution Spectra

Spectra of samples in aqueous solutions were measured with a Bruker Optics RAM II module coupled to a Bruker Optics Vertex 70 FT-IR spectrometer. The RAM II module was equipped with a high sensitivity germanium detector (D-418 TF) cooled by liquid nitrogen and a diode pumped 500 mW Nd:YAG laser (wavelength: 1064 nm). Data acquisition and analysis was performed using the software package OPUS 5.4 from Bruker Optics. The laser power was set to a value 500 mW for recording the solution spectra and up to 4000 scans were collected. Optimal concentrated solution samples were made preparing complex solutions with concentrations ≥ 0.15 mol/l in deionised water which were transferred into a one side mirrored quartz sample cell for Raman measurements.

2. Computational Aspects

The geometries of the conformational isomers **tb** and **hc** of [Fe(tmdta)]⁻ (high-spin) in the gas phase were fully optimized using the B3LYP hybrid density functional^{8,9} in combination with a 6-31+G* basis set¹⁰ with pure d and f functions in the spin-unrestricted formalism. C_2 symmetry was applied to the **tb** conformer, whereas the **hc** conformer was regarded to be not symmetric. The obtained structures (the Cartesian coordinates are listed in Table S3) were characterized to be energy minima by calculating analytical force constants in the harmonic approximation.

The same method was used to calculate vibrational spectra. Raman activities were obtained by numerical differentiation of analytic dipole derivatives with respect to an electric field. The vibrational frequencies were used unscaled to obtain the thermal corrections for total energies via statistical thermodynamics at 298 K and 1 atm. All calculations were carried out using the Gaussian 03 program package¹⁰ on an IBM p690 cluster (HLRN)¹¹.

For suitable comparison with the experimental spectra, a scale factor of 1.027 has been applied (cf. Table 1). This type of approach is a common practice for comparisons between computed and experimental spexcctra.¹²⁻¹⁴

The assignment of the bands listed in Table 1 was based on analysis of the corresponding atomic motions. When possible, i.e. when coupling between elementary displacements was limited, the band was assigned to a single specific displacement, such as the (Fe–N) stretching vibrations.

Table S3a. Cartesian coordinates for the optimized ***tb*** structure.

atom	x	y	z
Fe	-0.000296	0.581411	-0.085681
O	-0.319096	0.137647	-1.585364
O	-1.414344	-1.076843	1.5075589
O	-1.56223	1.698164	3.584522
O	-3.6837089	1.781324	-3.5197351
O	1.559296	1.704084	-0.577813
O	3.6788671	1.797583	0.298851
O	0.319321	0.120993	1.888888
O	1.41723	-1.1061831	-1.986268
N	-1.632814	-1.016908	0.008281
N	1.634802	-1.0121059	0.030544
C	-2.20135	-1.16611	-0.18221
C	-1.243711	-0.683239	0.242298
C	-2.5840099	-0.351285	-1.098395
C	-2.662466	1.1697429	-1.0786901
C	2.583684	-0.337509	0.989803
C	2.659488	1.1816961	1.118456
C	2.2050371	-1.170621	2.3910961
C	1.2459379	-0.70155	1.3371381
C	-1.132267	-2.283731	-2.3883419
C	0.00358	-3.028249	-1.288324
C	1.135888	-2.2753911	0.749382
H	-2.500901	-2.202244	-0.02432
H	-3.1037731	-0.550008	-1.2268699
H	-3.5882249	-0.790245	0.932027
H	-2.2148631	-0.478234	-0.719007
H	3.5888131	-0.775018	-2.0370059
H	2.2137301	-0.457161	-0.983807
H	2.5095119	-2.207062	2.0765669
H	3.1046009	-0.550972	1.122488
H	-0.800751	-2.04177	1.25897
H	-1.971529	-2.9936359	1.679979
H	-0.429812	-3.692704	-1.281823
H	0.439941	-3.6944959	-1.512587
H	0.801794	-2.026365	1.763087
H	1.976503	-2.9826181	0.836867

Table S3b. Cartesian coordinates for the optimized *hc* structure.

atom	x	y	z
Fe	-0.037072	0.496808	-0.003586
O	-3.6732669	1.328764	1.9165421
O	3.3185301	1.997481	3.466933
O	-1.485508	-0.625432	-0.352281
O	1.600618	-1.039165	-1.112748
O	-1.659608	1.474287	0.337062
O	1.431852	1.7328449	1.1016591
O	-0.262965	0.221277	-1.919638
O	0.240709	-0.095175	-3.4581449
N	-1.601006	-1.129594	-0.151624
N	1.791059	-0.902259	0.159295
C	-1.020012	-2.4782259	1.2077661
C	1.555328	-2.359971	2.314949
C	-2.67257	0.8216	-1.0768321
C	-2.5177951	-0.716903	-0.829115
C	2.4605401	1.2967989	1.08032
C	2.5467761	-0.242295	0.820679
C	-1.265254	-0.434895	-1.198289
C	-2.2411439	-0.984863	-2.3100929
C	1.359956	-0.625701	-0.732183
C	2.433136	-0.678343	0.010023
C	0.169791	-2.7967539	0.748803
H	-1.810734	-3.231256	1.406724
H	-0.701286	-2.5523939	1.288476
H	2.3209629	-2.745707	-1.01129
H	1.724118	-2.858238	-2.099215
H	-2.077477	-1.006191	1.0191751
H	-3.5061309	-1.1862431	2.103282
H	2.094995	-0.514327	-1.388037
H	3.6029739	-0.547257	-1.283566
H	-3.060492	-0.263028	-1.7418979
H	-2.6710711	-1.935014	-0.835822
H	2.934845	0.293995	0.768959
H	3.1846349	-1.445671	-0.745617
H	-0.010974	-2.42974	1.755954
H	0.225071	-3.8911729	0.859638

References

- 1 J. A. Weyh and R. E. Hamm, *Inorg. Chem.*, 1968, **7**, 2431-2435.
- 2 A. Fischer, *Acta Crystallogr.*, 2006, **E62**, i94-i95.
- 3 R. Nagao, F. Marumo and Y. Saito, *Acta Crystallogr.*, 1972, **B28**, 1852-1856.
- 4 T. Yamamoto, K. Mikata, K. Miyoshi and H. Yoneda, *H. Inorg. Chim. Acta*. 1988, **150**, 237-244.
- 5a H. P. Bommeli, G. Anderegg and W. Petter, *Z.Kristallogr.* 1986, **174**, 23; H. P. Bommeli, *Dissertation thesis*, ETH Zürich 1992.
- 5b K.-I. Okamoto, K. Kanamori and J. Hikada, *Acta Crystallogr.*, 1990, **C46**, 1640-.
- 6 H. Weakliem and J. L. Hoard, *J. Amer. Chem. Soc.*, 1959, **81**, 549-555.
- 7 R. Meier, M. Molinier, C. Anson, A. K. Powell, B. Kallies and R. van Eldik *Dalton Trans.*, **2006**, 5506-5514.
- 8 A. D. Becke, *J. Chem. Phys.*, 1993, **97**, 5648–5652; C. Lee, W. Yang and R.G. Parr, *Phys. Rev. B*, 1988, **37**, 785–789.
- 9 P. J. Stephens, F. J. Devlin, C. F. Chabalowski and M. J. Frisch, *J. Phys. Chem.*, 1994, **98**, 11623–11627.
- 10 Gaussian 03 (Revision B.05), M. J. Frisch, G. W. Trucks, H. B. Schlegel, G. E. Scuseria, M. A. Robb, J. R. Cheeseman, J. A. Montgomery, Jr., T. Vreven, K. N. Kudin, J. C. Burant, J. M. Millam, S. S. Iyengar, J. Tomasi, V. Barone, B. Mennucci, M. Cossi, G. Scalmani, N. Rega, G. A. Petersson, H. Nakatsuji, M. Hada, M. Ehara, K. Toyota, R. Fukuda, J. Hasegawa, M. Ishida, T. Nakajima, Y. Honda, O. Kitao, H. Nakai, M. Klene, X. Li, J. E. Knox, H. P. Hratchian, J. B. Cross, C. Adamo, J. Jaramillo, R. Gomperts, R. E. Stratmann, O. Yazyev, A. J. Austin, R. Cammi, C. Pomelli, J. W. Ochterski, P. Y. Ayala, K. Morokuma, G. A. Voth, P. Salvador, J. J. Dannenberg, V. G. Zakrzewski, S. Dapprich, A. D. Daniels, M. C. Strain, O. Farkas, D. K. Malick, A. D. Rabuck, K. Raghavachari, J. B. Foresman, J. V. Ortiz, Q. Cui, A. G. Baboul, S. Clifford, J. Cioslowski, B. B. Stefanov, G. Liu, A. Liashenko, P. Piskorz, I. Komaromi, R. L. Martin, D. J. Fox, T. Keith, M. A. Al-Laham, C. Y. Peng, A. Nanayakkara, M. Challacombe, P. M. W. Gill, B. Johnson, W. Chen, M. W. Wong, C. Gonzalez and J. A. Pople, Gaussian, Inc., Pittsburgh PA, 2003.
- 11 Norddeutscher Verbund für Hoch- und Höchstleistungsrechnen (HLRN), <http://www.hlrn.de> 2003.
- 12 A. Stirling, *J. Chem. Phys.*, 1996, **104**, 1254.
- 13 M. Lazzeri and F. Mauri, *Phys. Rev. Lett.*, 2003; **90**, 036401
- 14 S. Loridant, M. Digne, M. Daniel and T. Huard, *J. Raman Spectrosc.*, 2007, **38**, 44-52.